

THE ELECTRON BEAM FOR THE FERMILAB ELECTRON COOLING EXPERIMENT

W. B. Herrmannsfeldt,* W. Kells,† P. M. McIntyre,† F. Mills,† J. Misek,† and L. Oleksiuk†

Abstract

We describe the design and construction of the electron beam for the Fermilab Electron Cooling Experiment. Important parameters are (1) 110 keV kinetic energy; (2) 26 A current; (3) 0.5 eV rest frame temperature; (4) space charge neutralization; (5) beam modulation; (6) efficient energy recovery at the collector. The 5 m overlap region between the electron beam and the storage ring orbit represents 4% of the total ring circumference.

Introduction

An electron beam has been designed and built for the Fermilab Electron Cooling Experiment. Its optical quality is compatible with optimum cooling of a "hot" 200 MeV proton beam which fills the acceptance of the storage ring. The expected cooling rate for such a proton beam is 3 Hz; a cooling rate of 15 Hz can be accommodated by beam modulation and/or by extending the drift section of the electron beam.

General Features of the Electron Beam

Table I lists the appropriate electron beam parameters. The electron beam matches velocity with the proton beam, so that (in the mean) they share a common rest frame. A high-perveance spherical Pierce cathode is immersed in a converging longitudinal magnetic field. The beam emerges from the extraction anode into a set of electrostatic electrodes designed to act as a resonant-focusing triplet.

The beam is then bent 90° into alignment with the proton beam and traverses a 5 m drift region where cooling occurs. It is then bent 90° and enters a decelerating structure similar to the gun region.

The electron beam is decelerated to about 5 keV energy and collected on a water-cooled collector assembly. The total dissipated electron beam power is thus ≤ 130 kW.

Table I. Electron Beam Parameters

Beam density	1.5 A/cm ²
Beam diameter	5.1 cm
Gun perveance ($I/V^{3/2}$)	2.27 μ perva
Cathode temperature	0.1 eV
KE, β , γ	110 kV, .57, 1.21
Nom. guide field	~ 1000 G

*Stanford Linear Accelerator Center, Stanford, California; operated by Stanford University, under contract with the United States Department of Energy.

†Fermi National Accelerator Laboratory, Batavia, Illinois; operated by Universities Research Association, Inc., under contract with the United States Department of Energy.

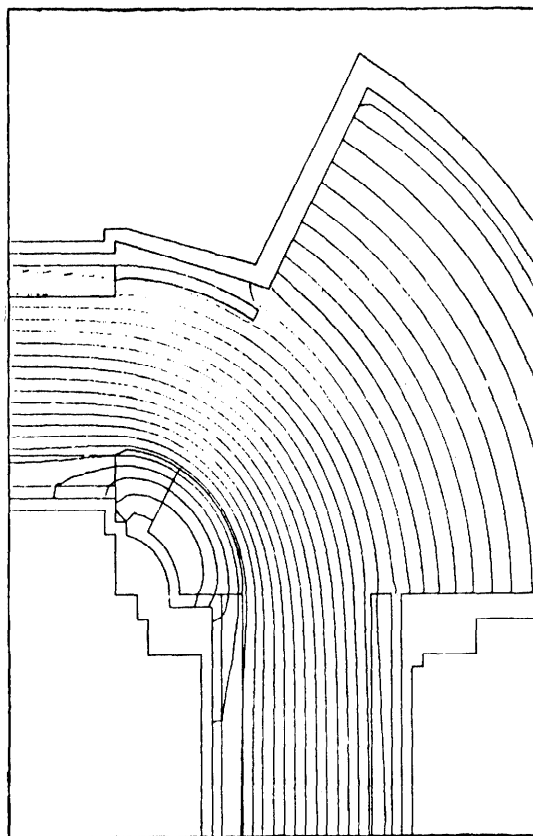


Fig. 1. Computer modeled flux distribution in toroid region.

Magnetic Field Design

The magnetic field lines converge in the gun region to follow closely the space-charge-defined electron trajectories. The electron beam leaves the gun section vertically and is then deflected through 90° to the horizontal by means of a toroidal magnetic field $B(r) = B_0 R/r$, where $B_0 = 1$ kg at $R = 0.5$ m. In addition a transverse dipole field of 25 G is added so that the electrons freely follow the curvature of the toroidal field without exciting spiral motion.

The guide field in the cooling region is produced by a set of five 1 m long solenoidal coils constructed of anodized aluminum strip conductor. Additional correction coils are provided to compensate for the 3 mm gaps between the main coils. Because the cooling process occurs in this region, magnetic field uniformity design goals were held to

$$\left| \frac{\Delta B}{B} \right|_{\text{rms}} < 1 \times 10^{-3}$$

corresponding to an electron transverse temperature $T_{\perp} < 1 \text{ eV}$.¹ The field direction has been aligned among the five solenoid sections to an rms accuracy of 0.2 mrad, by adjusting the independent mechanical suspension of each section. The magnetic boundary reluctance paths have been balanced so that the on-axis flux line leaving the cathode would land on the cooling section geometrical axis and also on the collector axis, to an accuracy of $\sim 1 \text{ mm}$.

Figure 1 shows the computer-modeled flux distribution calculated in the toroidal region. The axial flux lines are predicted to droop radially inward from the geometrical axis by about 16 mm within the toroidal region due to the mismatch between the solenoidal and toroidal field distributions.

The actual flux line paths were measured by using a 200 μA low energy ($\sim 1 \text{ kV}$) electron beam to follow actual flux paths under nominal operating fields. The probe beam position was measured (to within $\pm 0.002''$) in the long solenoid by observing a phosphor screen with an alignment telescope, and in the toroid and gun region by current division from a resistive plate which was driven on a circular arc through the toroidal region. Flux line position resolution of $\sim 0.1 \text{ mm}$ was possible with this technique.

In addition magnetic field maps using Hall probe instrumentation were performed to monitor the field uniformity. These studies enabled various corrections to be made for smoothing out flux density perturbations. Figure 2 shows the results of field magnitude smoothing corrections in the solenoid section.

Table II lists the operating values of various magnetic system components.

Table II. Electron Beam Guide Field Components

Element	Field	Function
200" Main Solenoid	$B_z = 1000 \text{ G}$	guide field in cooling section
90° Toroid	$B(r) = B_0 R/r$, $B_0 = 1000 \text{ G}$, $R = 0.5 \text{ m}$	bend electron beam into/away from proton beam
20" Gun/Collector Solenoid	$B_z = 900 \text{ G}$	match electron beam from cathode to guide field
6" End Pack Solenoid	$B_z(\text{max}) = 150 \text{ G}$	fine matching of beam to gun focusing section
Gap correction Coils	$B_z(\text{max}) = 9 \text{ G}$	correct for gaps in main solenoid
Transition Coils (3)	$B_z = 10\text{-}20 \text{ G}$	matching solenoid-toroid transition regions
Toroid Drift Dipole	$B_s = 25 \text{ G}$	cancel drift in toroid region
Alignment Dipoles	$B_x = B_y \approx 20 \text{ G}$	align electron beam axis to proton beam axis

The Gun Region

The major constraint in the magnetic field design was to maintain the transverse

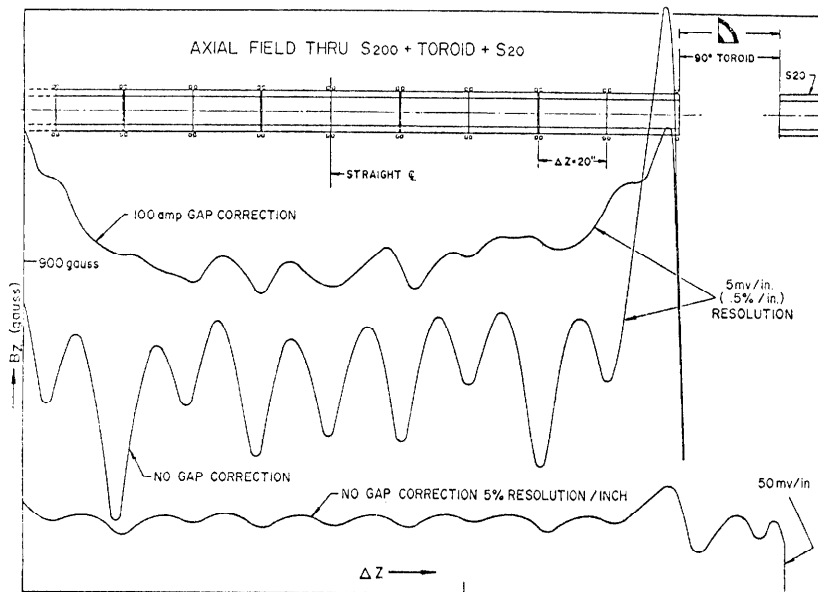


Fig. 2. Measured guide field non-uniformity and corrected guide field.

beam temperature below 1 eV in the cooling region.

Though the initial temperature of the electron beam leaving the cathode is about 0.1 eV, space charge forces would quickly increase this temperature to a few keV after leaving the Pierce geometry. By controlling the flux convergence in this region, we can control the transverse motion. The total gun design takes into account the relation of the crossed electric and magnetic fields, and the gyro-wavelength for transverse motion. The electrostatic lenses are spaced at the gyro-wavelength, so that the gun can produce a transversely cool beam ($T_{\perp} \lesssim 1$ eV) independent of the beam current.

The calculations for the gun design used a computer code² to model the trajectories of the electrons with the measured magnetic and electric field distribution. Of particular importance is the transverse velocity along each trajectory. Control of T_{\perp} in the drift region is the essence of a proper matching algorithm needed to tune the gun. Figure 3 shows the typical gun geometry for a 26 A x 110 kV beam where the beam travels about 1/2 m to the toroidal region.

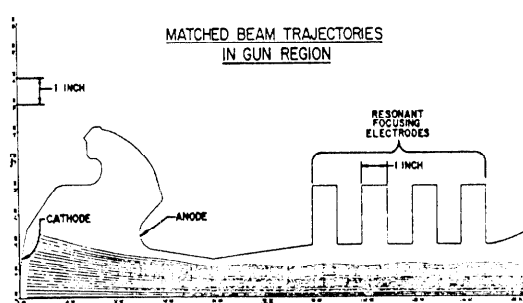


Fig. 3. Computer gun modeling of 110 kV trajectories at high currents.

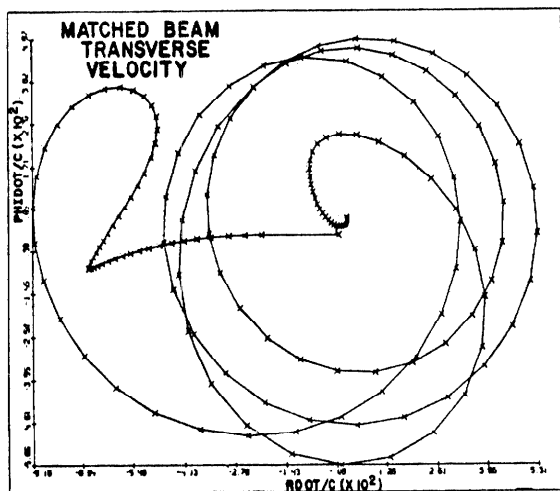


Fig. 4. History of transverse temperature for beam-edge electron in gun region.

Figure 4 shows the history of transverse velocity for a trajectory near the beam edge.

This plot demonstrates how proper tuning of the accelerating fields results in a "cool" transverse temperature as the beam leaves the gun region.

The Solenoid and Toroid Region

Further computer studies of the effects of the periodic gap perturbation in the main solenoid field indicate that the measured field uniformity is sufficient to control the beam transverse energy to $T_{\perp} < 0.25$ eV. In the transition region between solenoid and toroid, the field is neither uniform nor toroidal, and the electron trajectories are perturbed radially. The effect on transverse temperature can be largely removed by scaling the guide field intensity so as to cancel the effects in the two transition regions of each toroid. To do this we require that a half-integral number of gyro-wavelengths separate the transition perturbations. This requires phase coherence in the gyro-motion across the profile of the beam as it traverses the toroid. The gyro-wavelength is

$$\lambda(r) = \beta c / \omega, \text{ where } \omega = eB(r) / mc = eB_0 R / mcr$$

is the gyro-frequency. The path length through an angle θ of the toroid is $s(r) = \theta r$. The phase advance ϕ of gyro-motion is thus independent of the radius r of an electron trajectory:

$$\phi = 2\pi s / \lambda = 2\pi e B_0 R \theta / \beta m c^2.$$

We can clearly choose the guide field B_0 such that $\phi / 2\pi = n + 1/2$ for the effective separation angle θ between transition perturbations; the beam will then emerge "cool" into the drift region.

Additional trim coils have been installed to permit matching the on-axis trajectory from the gun to the drift region to the collector.

The Collector Region

The collector region has been designed as an approximate mirror image of the gun region. This feature allows complete control of the transverse beam energy when the beam is dumped. For efficient low energy collection ($\lesssim 5$ kV) no longitudinal energy must be lost to the gyro-motion. This is vitally important since space charge potential islands can slow some trajectories to ~ 1 kV before they reach the 5 kV collector surface.

Suppression of secondary emission is difficult near the beam edge. In this region studies are underway to design suppression field electrodes. It is anticipated that $\lesssim 10^{-3}$ of the primary beam will be lost from collection when all fields have been optimized.

Space Charge Neutralization

Electron cooling can be enhanced in a region of strong magnetic field, because the electron is no longer free to recoil from a proton during the cooling process. The enhancement factor F is simply the number of electron spirals that occur while the electron and proton are still within a longitudinal distance of a gyro-radius ρ .

$$F = 1 + \rho_g \omega_g / 2\pi v_{||} = 1 + \sqrt{T_{\perp} / T_{||}} / 2\pi .$$

When $T_{||} \ll T_{\perp}$, this coherence dominates the cooling process. Enhancements of a factor $F \sim 8$ have been observed in the cooling experiments at Novosibirsk.³

The "natural" longitudinal temperature is cooled in the acceleration kinematics:

$T_{||} \approx T_0 \left(\frac{T_0}{4V} \right)$ where $T_0 \sim$ few eV is due to fluctuations in the beam kinetic energy V . This yields $T_{||} \sim 10^{-5}$ eV $\ll T_{\perp}$. In practice, the longitudinal temperature is determined by the space charge depression $\delta V \approx 1200$ V across the beam profile: $T_{||} \sim (e\delta V / \beta\gamma mc^2)^2 = 1$ eV $\sim T_{\perp}$.

In order to make coherent cooling possible, we must neutralize the space charge in the cooling region. This will be accomplished by creating a potential well of several kV in the cooling section by means of drift tubes surrounding the beam.

The required ion density for space charge neutralization corresponds to a pressure 2×10^{-8} Torr for hydrogen.

Acknowledgements

We would like to express our thanks to D. Rogers of Teledyne MEC for generously providing us with a probe gun source. We also wish to acknowledge the dedication of the Fermilab Internal Target technical group in the execution of the gun design and construction.

References

1. Fermilab Electron Cooling Experiment Design Report, August 1978.
2. W. B. Herrmannsfeldt, Electron Trajectory Program, SLAC Report No. 166 (Sept. 1973).
3. G. I. Budker, N. S. Dikansky, V. I. Kudelaninen, I. N. Meshkov, V. V. Parkhomchuk, D. V. Pestrikov, A. N. Skrinsky, B. N. Sukhina, "Experimental Study of Electron Cooling", Particle Accelerators, v. 7, No. 4 (1976).